This is an *Accepted Manuscript*, which has been through the Royal Society of Chemistry peer review process and has been accepted for publication.

Accepted Manuscripts are published online shortly after acceptance, before technical editing, formatting and proof reading. Using this free service, authors can make their results available to the community, in citable form, before we publish the edited article. We will replace this *Accepted Manuscript* with the edited and formatted *Advance Article* as soon as it is available.

You can find more information about *Accepted Manuscripts* in the Information for Authors.

Please note that technical editing may introduce minor changes to the text and/or graphics, which may alter content. The journal's standard Terms & Conditions and the Ethical guidelines still apply. In no event shall the Royal Society of Chemistry be held responsible for any errors or omissions in this *Accepted Manuscript* or any consequences arising from the use of any information it contains.

Hydrogenation of oxalic acid using light-assisted water electrolysis for the production of an alcoholic compound

Sho Kitano[a], Miho Yamauchi[a]*, Shinichi Hata[a], Ryota Watanabe[a], Masaaki Sadakiyo[a],

[a]International Institute for Carbon-Neutral Energy Research (WPI-I2CNER), Kyushu University, Motooka 744, Nishi-ku, Fukuoka 819-0395, Japan.

CORRESPONDING AUTHOR

Dr. Miho Yamauchi

Associate Professor, International Institute for Carbon-Neutral Energy Research (WPI-I2CNER), Kyushu University, Motooka 744, Nishi-ku, Fukuoka 819-0395, Japan.

Phone: +81-92-802-6874. E-mail: yamauchi@i2cner.kyushu-u.ac.jp

We demonstrate the production of glycolic acid, an industrially important alcoholic compound, via the electrochemical reduction of oxalic acid, which is procurable from biomass, and electro-oxidation of water with the help of renewable light energy for the first time. In principle, this new synthesis system is achievable while minimizing the consumption of fossil resources. We built a precious-metal free electrosynthesis system by employing a TiO_2 cathode for oxalic acid reduction and a WO_3 photoanode for water oxidation. The alcohol production proceeds during the application of electric power above 2.1 V in the dark. Notably, UV-visible light irradiation of the WO_3 photoanode enables glycolic acid electrosynthesis above 0.5 V, which is lower (by 0.6 V) than the theoretical bias, i.e., 1.1 V. The glycolic acid electrosynthesis with an 80% high Faradaic efficiency was achieved when applying a bias of 1.5 V under UV-visible irradiation ($\lambda > 300$ nm).
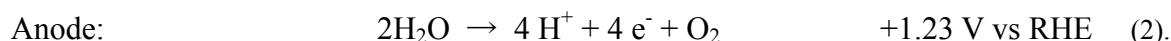
1   Currently, the chemical industry largely depends on fossil fuels, which serve not

2   only to generate power but also as hydrogen and carbon sources; fossil fuels are also

3   believed to be a contributing factor to the global warming due to the increase of CO_2

4   concentrations. Efficient utilization of biomass resources derived from atmospheric CO_2

5   could be a useful strategy to curbing global warming by suppressing the consumption of

6   fossil resources as a raw material.[1-4] Recently, bio-alcohols, such as ethanol[5] and ethylene

7   glycol,[6] have been commercialized and utilized as a fuel[7] and feedstock.[8] However, carbon

8   resources included in biomass are not efficiently converted into alcohols, i.e., the carbon

9   yield in the bio-alcohol production through fermentation is not beyond 50% and the

10   residual carbon is released back into the air.[9] Besides, the low production rate is due to the

11   slow enzyme reaction.[10]

12   Catalytic hydrogenation of carboxylic acids has attracted much attention as a novel

13   synthetic route for the production of alcoholic compounds from bio-derived materials.[11]

14   Several groups have succeeded in the catalytic hydrogenation of organic acids, such as

15   acetic acid,[12] stearic acid[13] and aromatic carboxylic acid,[14, 15] to produce corresponding

16   alcoholic compounds. However, severe reaction conditions are required for the catalytic

17   hydrogenation of organic acids, i.e., high pressure (2-6 MPa) and temperature (100-380

18   $^oC)^{[15]}$ with use of H_2 gas. The other drawback of the organic hydrogenations process is the

19   utilization of highly reactive metal hydrides derived from fossil fuels as a hydrogen source,

20   e.g., $LiAlH_4,^{[16]}$ $(BH_3)_2^{[17, 18]}$ and $HSiEt_3,^{[19]}$ to activate highly stable carboxyl groups due to

21   their low electrophilicty[20] in organic solvents, resulting in the formation of large amounts of

22   waste.[21]

23   Alternatively, light-energy-driven electrochemical water splitting using a

24   photoelectrode, such as oxide,[22-27] (oxy)nitride[28-31] and sulfide[32] is regarded as a clean

25   process for producing hydrogen from water using renewable solar energy and for providing

1   an effective means of energy storage. In this study, we focus on the utilization the hydrogen

2   generated photocatalytically from water in chemical syntheses and photovoltaic effects to

3   accelerate electrochemical reactions. Thus, the electrochemical reduction of carboxylic

4   acids using water as a hydrogen source with the assistance of light energy would achieve

5   the highly efficient hydrogenation of carboxylic acid with fossil-free hydrogen, i.e.,

6   *light-energy-driven alcohol synthesis from fossil-free carboxylic acid and water*, as

7   shown in Fig. 1. This process is expected to become an excellent, environmentally friendly

8   alcohol production route, if it progresses under largely milder conditions (0.1 MPa, <100

9   ^{o}C) than those of hydrogenation reactions.

10   Previously, we have demonstrated the electrochemical reduction of oxalic acid,

11   $(COOH)_2$,**OX**, a divalent carboxylic acid, to produce glycolic acid, $HOOC\text{-}CH_2OH$, **GC**,

12   an alcoholic compound (α-hydroxy carboxylic acid)[33] through the 4-electron reduction of

13   **OX** with oxidation of water as described in equation 1-3.

14   Cathode: $(COOH)_2 + 4\,H^{+} + 4\,e^{-} \rightarrow HOOC\text{-}CH_2OH + H_2O$ +0.13 V vs RHE   (1).

15   Anode: $2H_2O \rightarrow 4\,H^{+} + 4\,e^{-} + O_2$ +1.23 V vs RHE   (2).

16   Overall: $(COOH)_2 + H_2O \rightarrow HOOC\text{-}CH_2OH + O_2$ 1.1 V   (3).

17   The **OX** is first reduced to GO (HOOC-COH, GO) through two-electron reduction, and

18   then **GC** is produced from GO through further two-electron reduction [34, 35] (see the scheme

19   S1 in ESI†). The **GC** formation was found to proceed with high selectivity (>98%) and

20   Faradaic efficiency (>95%) in an electrochemical cell equipped with a titanium (IV)

21   dioxide (TiO_2) cathode for **OX** reduction and a Pt wire anode for water oxidation, which

22   corresponds to a direct electric power charge into an alcoholic compound.

23   Furthermore, in this study, a light-assisted electrochemical alcohol production

24   system was fabricated by adapting oxide semiconductor photoelectrodes as the anode for

25   water oxidation to supply protons and electrons for the hydrogenation of a carboxylic acid,

1   which enables the direct conversion of light energy into low-carbon alcoholic chemicals.

2   Here, we applied Ga_2O_3,[36, 37] $BiVO_4$[38] and WO_3[24, 39] particles, which are known as highly

3   active photocatalysts for water oxidation, as the photoanode to oxidize water and to provide

4   electrons and protons for the electro-reduction of **OX** on an anatase-type TiO_2 cathode

5   under UV-visible light irradiation. We successfully produced **GC** from **OX** through an

6   electrochemical reaction in the remarkably low bias potential range, i.e., ~1.5 V, compared

7   with the potentials without light irradiation, ~2.5 V.

8   Commercially supplied Ga_2O_3 and WO_3 powders were used in the electrochemical

9   experiments. The $BiVO_4$ powders were prepared by using the homogeneous-precipitation

10   method according to a previous report (see the Experimental section in ESI†).[40] All samples

11   were characterized by X-ray powder diffraction (XRD) and UV-visible diffuse reflection

12   measurements. The Ga_2O_3, $BiVO_4$ and WO_3 powders showed XRD patterns attributable to

13   monoclinic structures and photoabsorption spectra, which coincide with the structure and

14   spectrum of materials reported as highly active photocatalysts for O_2 evolution by water

15   splitting (Figs. S1 and S2†).[24, 36-40] Anodes were prepared by applying a suspended mixture

16   of water, acetylacetone (disperser), Toriton-X (thickener) and the oxide powders on

17   conductive glass using a squeegee method,[41] followed by calcination at 450°C for 4 h. The

18   TiO_2 cathode was prepared by drying a methanolic suspension of TiO_2 nanoparticles (Japan

19   Reference Catalyst of TiO_2: JRC-TIO-8, an anatase-type TiO_2) dropped onto Ti foil,

20   followed by calcination at 450°C for 0.5 h. Two-electrode systems were equipped using

21   two-compartment cells, where the cathode and anode were separately mounted in each cell

22   to evaluate an applied bias for **OX** reduction without re-oxidation of the reduced product at

23   the anode as shown in Fig. 1. All electro-reduction experiments were conducted by

24   introducing 0.16 M **OX** cathode solution containing 0.16 M Na_2SO_4 (pH 1.2) and 0.16 M

25   Na_2SO_4 anode solution (pH 5.8) at 25°C. Fig. 2 and Fig. S3† show the current-voltage

1　curves for the electro-reduction of **OX** on Ga_2O_3, $BiVO_4$ and WO_3 photoanodes in the dark,

2　and under UV-visible light (λ > 200 nm) irradiation. We could observe reductive currents

3　on all three anodes by applying external bias above 2.1 V in the dark, as shown in Fig. 2 ,

4　indicating that the application of 1.0 V as a total over potential, in addition to 1.1 V of the

5　theoretical cell voltage (equation 3), is a requisite for initiating the **GC** production through

6　**OX** reduction and water oxidation without light irradiation. Under light irradiation,

7　minimal biases applied to flow reductive current in the system were drastically decreased

8　compared with those observed in the dark. These results clearly indicate that the external

9　applied bias can be enhanced by photoirradiation, causing photoexcitation over

10　photoanodes absorbing UV-visible light energy. The chemical bias in the two-electrode

11　system employing cathode (pH=1.2) and anode (pH=5.8) solutions is calculated to be 0.27

12　V based on the following equation:

$$\text{Chemical bias (V)} = 0.059 \times |pH_{anode} - pH_{cathode}| = 0.27 \text{ V}$$

13　Thus, we can beneficially utilize the chemical bias to lower the applied bias required for the

14　reactions. On the other hand, we conducted **OX** reduction experiments both under light

15　irradiation and in the dark to investigate the effects of light irradiation on the applied bias

16　under the same experimental conditions. In acidic aqueous solutions having pH < 2, the

17　photoanode composed of Ga_2O_3 or $BiVO_4$ dissolves and photocatalytic oxidation of

18　co-existing electrolyte anions, SO_4^{2-}, proceeds on the WO_3. Dissolution of the WO_3 also

19　occurs in strong alkaline solutions. Thus, in this study, we utilize an aqueous solution of

20　Na_2SO_4 without pH control, which exhibits neutral pH condition, for the efficient water

21　oxidation reaction.

22　　　　The onset potential for the reductive current flow under UV-visible irradiation light

23　depended on the photoanodes; the order of onset bias was as follows: WO_3 < $BiVO_4$ <

24　Ga_2O_3. This order coincides with the photovoltaic performance of photoanodes, i.e., WO_3 >

1   BiVO$_4$ > Ga$_2$O$_3$. An observed decrease of the onset biases for the electro-reduction of **OX**

2   is therefore associated with the photovoltaic performance, which depends on the amount of

3   optically excited electrons and holes and recombination probabilities between such excited

4   species, and correspond to the activity of photoanodes for water oxidation. Photoexcitation

5   probabilities for the generation of active specie strongly depend on the range of

6   photoabsorption wavelengths of photoanodes.[42] A wider absorption range of the

7   photoanodes achieves more efficient photoexcitation within the entire irradiation range (λ >

8   200 nm), generating a larger amount of excited electrons and holes. All excited electrons

9   and holes, however, are not available because the recombination between some parts of

10   electrons and holes occurs before the water oxidation proceeds.[43] Lower recombination

11   probability enables higher reaction probability of holes and water molecules, resulting in

12   higher activity of water oxidation and a larger amount of available excited electrons, i.e.,

13   higher photovoltaic performance.[44] Therefore, the photoanode, which shows a wide

14   photoabsorption spectrum and low recombination probability, is expected to exhibit large

15   bias decrease due to the high activity for water oxidation and photovoltaic performance.

16   The Ga$_2$O$_3$ photoanode exhibited the smallest bias decrease under light irradiation

17   (0.15 V, as shown in Fig. 2) because the narrowest range of photoabsorption wavelengths of

18   the Ga$_2$O$_3$ photoanode (up to 270 nm, as shown in Fig. S2†) corresponds to the smallest

19   amount of excited electrons and holes (as illustrated in Fig. 2), thus, resulting in the low

20   activity for water oxidation and photovoltaic performance. Although the BiVO$_4$ photoanode

21   showed the widest absorption spectrum (up to 550 nm) of all the photoanodes, **OX**

22   reduction over the photoanode required the application of a relatively high bias potential,

23   i.e., 1.7 V, compared with 0.7 V, which was observed over the WO$_3$ anode. This observation

24   clearly shows that the recombination probability is more crucial for water oxidation over

25   the BiVO$_4$ anode. It is known that the BiVO$_4$ photoanode shows a high recombination

1　probability due to its poor mobility for excited electrons (Fig. 2).[45-48] By contrast, the WO_3

2　photoanode, absorbing photons at wavelengths less than 480 nm, exhibited the largest bias

3　decrease of all the anodes, as shown in Fig. 2 and Fig. S2†. Therefore, the largest decrease

4　of applied bias for **OX** reduction observed on the WO_3 photoanode can be attributed to the

5　relatively wide absorption spectrum and low recombination probability for efficient water

6　oxidation and high photovoltaic performance.[24]

7　Reaction conditions of the most active WO_3 catalyst were optimized to minimize the

8　applied bias by changing pH values over the anode and cathode to achieve efficient alcohol

9　electrosynthesis. For this purpose, a three-electrode system, as described in Fig. S4†, was

10　applied to determine an applied potential on the TiO_2 cathode by comparing the cathode

11　potential with a reference electrode potential, whereas we could measure the bias applied

12　between a cathode and an anode in the two-electrode system. Electrochemical cells were

13　filled with Na_2SO_4 aqueous solution (40 ml, 0.2 M) and the pH value in the cathode cell

14　including **OX** (0.03 M) was controlled to be either 1.0 or 11 by adding H_2SO_4 or NaOH

15　solution. TiO_2 is known as a sufficiently stable oxide compound in both acidic and alkaline

16　conditions and the TiO_2 cathode stably worked during catalytic experiments conducted in

17　this study.

18　Fig. S5† shows the influence of the pH value on the activity for **OX** reduction and a

19　product distribution in chronoamperometric electro-reduction with application of a constant

20　cathode potential, i.e., -0.7 V vs the reversible hydrogen electrode (RHE) at 50°C for 2 h.

21　At pH values higher than or equal to 7, we could not observe any reduction products, i.e.,

22　0% **OX** conversion. Decreasing the pH value to less than or equal to 4 led to the generation

23　of both 2- and 4-electron reduction products, i.e., GO and **GC**, respectively; yields of both

24　reduction products and the percentage of **GC** yield increased with decreasing pH value.

25　Considering that the production of **GC** and GO are attained via the hydrogenation of **OX**, a

1 higher proton concentration under lower pH conditions confers a favorable condition for

2 the hydrogenation reaction.[49]

3 The influence of the wavelength of irradiation light on the WO_3 anode were

4 examined by applying a two-electrode system, which comprised a TiO_2 cathode in a

5 solution containing **OX** (0.03 M) and Na_2SO_4 solution (pH 1.0, 40 ml, 0.2 M) and a WO_3

6 photoanode in a Na_2SO_4 solution (pH 5.6, 40 ml, 0.2 M) at 50°C. Fig. 3 shows the

7 current-voltage curves both in the dark and under the irradiation of light of various

8 wavelengths, such as UV-visible light with $\lambda > 200$ and 300 nm and visible light with $\lambda >$

9 400 nm. We observed onsets of approximately 0.5 V under the irradiation of light at all

10 tested wavelengths, which are 0.6 V smaller than the theoretical bias required for **GC**

11 production via **OX** reduction and water oxidation, i.e., 1.1 V, whereas the onset potentials

12 were observed at approximately 2.1 V in the dark, suggesting that the remarkable bias

13 decrease of 1.6 V was attained by light irradiation. Irradiations of light with $\lambda > 200$ nm and

14 300 nm cover wide energy regions of absorption spectrum of WO_3. Therefore, the rate

15 determining-step for **OX** reduction under UV-visible light irradiation is probably not the

16 water oxidation over the WO_3 anode, where holes with sufficient positive potentials[50] are

17 generated, but the electro-reduction of **OX** on the cathode. Thus, we conclude that the

18 irradiation of UV-visible light with $\lambda > 300$ nm efficiently works in the system.

19 Furthermore, almost the same onset potential of reductive current was observed under

20 visible light irradiation, indicating that the WO_3 photoanode could efficiently work for the

21 bias decrease under visible light irradiation. These results indicate that the system has

22 applicability under both the irradiation of solar light and only visible light.

23 Chronoamperometric electro-reduction of **OX** was conducted while applying an

24 external bias of 1.0 or 1.5 V with a two-electrode system employing the TiO_2 cathode in

25 **OX** solution (pH 1.0, 40 ml, 0.03 M **OX**, 0.2 M Na_2SO_4) and the WO_3 photoanode in

1   Na_2SO_4 solution (pH 5.6, 40 ml, 0.2 M) at 50°C for 2 h under irradiation of UV-visible light

2   with λ > 300 nm, visible light with λ > 400 nm or in the dark. Fig. 4 shows the Faradaic

3   efficiencies calculated based on the amount of GO and **GC** produced under various

4   conditions. No products were detected in the dark even for an external bias below 1.5 V,

5   which is in accordance with the result that no reductive current was observed in the

6   current-voltage curve below 1.5 V, as shown in Fig. 3, and indicates that the system does

7   not work below 1.5 V without irradiation. By contrast, GO and **GC** production was

8   achieved under irradiations of both UV-visible and visible light, indicating that **OX** can be

9   reduced with the assistance of light energy absorbed by the WO_3 photoanode through an

10   electrochemical reaction system. Higher Faradaic efficiencies for GO and **GC** production

11   were achieved through the irradiation of UV-visible light and the application of a bias larger

12   than 1.5 V, compared with efficiencies under the irradiation of visible light at 1.0 V. Note

13   that GO and **GC** were produced with an 80% Faradaic efficiency in total when applying a

14   bias of 1.5 V under the irradiation of UV-visible light. The anode potential when applying a

15   bias of 1.5 V under the irradiation of UV-visible light was observed to be 1.05 V vs RHE,

16   which is 0.18 V more negative than the theoretical potential of water oxidation, 1.23 V vs

17   RHE, indicating that the hole generated by photoabsorption oxidized water molecules.[51, 52]

18   Furthermore, constant reductive-current flow at approximately 0.5 mA cm^{-1} was observed

19   with applying a bias of 1.5 V under the irradiation of UV-visible light for 2 h, except for the

20   initial period, as shown in Fig. S7†, indicating that the system can stably work and

21   reductive products are continuously obtained under the examined conditions. Gaseous

22   products generated in both cathode and anode cells were also analyzed to clarify the entire

23   Faradaic efficiency of the system. Fig. S8† shows the Faradaic efficiencies determined

24   based on the amount of GO, **GC** and H_2 that formed in the cathode cell in **OX** reduction

25   and O_2 that formed in water oxidation in the anode cell when applying a bias of -1.5 V

1   under the irradiation of UV-visible light. Faradaic efficiencies for products in each cell

2   reached 100%, indicating that the reaction substrates were only **OX** and water and all

3   electrons formed in water oxidation were consumed for the electro-reduction of **OX** or

4   water to produce GO, **GC** and H_2 through the circuit. H_2 generation occurred with low

5   evolution rate (7.9 μmol h^{-1}) as a side reaction of hydrogenation of **OX** when applying a

6   bias of 1.5 V of bias under irradiation of UV-vis light. In our electrochemical hydrogenation

7   system, protons and electrons are provided from electrolyte and electrode separately and

8   react with oxalic acids as shown in Scheme S1 (ESI†), resulting in glycolic acid production

9   without H_2 gas evolution. Therefore, the suppression of hydrogen evolution reaction (HER)

10   over a TiO_2 electrode is critically important to achieve high Faradaic efficiency for **OX**

11   reduction, which has been discussed in our previous report [33]. The TiO_2 electrode used in

12   this work also exhibited high activities for **OX** reduction but low HER activities in the

13   acidic condition, as reported in Nature Materials[53]. Based on these results, we succeeded in

14   the first production of alcoholic compound, **GC**, from carboxylic acid, **OX**, via water

15   oxidation using light energy through an electrochemical reaction system.

16   To improve of the product selectivity, we provide an illustration of the relation

17   between applied potentials on the TiO_2 cathode and Faradaic efficiencies for the

18   electro-reduction of **OX** to GO and **GC** in Fig. 5. The Faradaic efficiencies for GO and **GC**

19   production in the dark were determined using the three-electrode system, which comprised

20   a TiO_2 cathode and Ag/AgCl reference electrode in solution containing **OX** (0.03 M) and

21   Na_2SO_4 solution (pH 1.0, 40 ml, 0.2 M) and a Pt anode in Na_2SO_4 solution (pH 1.0, 40 ml,

22   0.2 M). Fig. 5 also shows the Faradaic efficiencies obtained using the two-electrode system

23   under the irradiation of UV-visible light with $\lambda > 300$ nm and visible light with $\lambda > 400$ nm,

24   which are displayed in Fig. 4. The Faradaic efficiencies depended on the TiO_2 cathode

25   potential and exhibited a volcano-like tendency regardless of the type of electrode system,

1   indicating that the TiO_2 cathode potential was the determining factor in the **OX** reduction

2   system. The highest Faradaic efficiency, i.e., 99%, was achieved at approximately -0.6 V vs

3   RHE in the three-electrode system. Fig. S9† shows cyclic voltammogram curves measured

4   using a three-electrode system employing a TiO_2 cathode, Pt anode and Ag/AgCl reference

5   electrode in the dark recorded in electrolyte solutions with and without the **OX** substrate,

6   respectively. The **OX** reduction current steeply increased below -0.45 V vs RHE, which

7   implicates the larger current density of **OX** reduction at -0.6 V vs RHE of the cathode

8   potential compared to that at -0.45 V vs RHE in the two-electrode system. On the basis of

9   the results, higher Faradaic efficiencies are also expected to be realized by the negative shift

10   of the cathode potential in the two-electrode system employing the WO_3 photoanode.

11   The performances for **OX** reduction in the light-assisted system were compared with those

12   of our previous work and other catalytic hydrogenation researches. The total yields and

13   reaction rates for GO and **GC** productions in this and previous works and results in the

14   reference 12-15 are summarized in Table S1. The total yields obtained using the

15   two-electrode system employing a standard TiO_2 catalyst in this work are relatively lower

16   than those in the references because of the smaller active sites on the surface of the standard

17   catalyst. On the other hand, the reaction rate using the three-electrode system employing

18   the highly active porous TiO_2 catalyst in our previous work is comparable with those in the

19   references, indicating that the utilization of highly active TiO_2 catalyst having the

20   sufficiently large reactive surface will probably achieve more efficient **OX** reductions.

21   In conclusion, we demonstrated **GC** production through **OX** electro-reduction and

22   water oxidation using a light-assisted electrochemical reaction system that applies a TiO_2

23   cathode and semiconductor oxide photoanodes. The reaction proceeds by applying a bias

24   potential of more than 2.1 V without light irradiation. Irradiation of UV-visible light to the

25   WO_3 photoanode enables a drastic decrease of minimal bias, i.e., 0.5 V, which is 0.6 V

1   smaller than the theoretical bias potential, i.e., 1.1 V, required for **GC** production via **OX**

2   reduction and water oxidation. **GC** electrosynthesis with an 80% Faradaic efficiency was

3   achieved when applying a bias of 1.5 V under UV-visible irradiation ($\lambda > 300$ nm). These

4   results are the first demonstration of a green synthetic process for the production of an

5   alcoholic compound from an organic acid procurable from biomass via electro-oxidation of

6   water with the assistance of light energy.

7

8

9

1   **References**

2   1.   G. W. Huber, S. Iborra and A. Corma, *Chem. Rev.*, 2006, **106**, 4044-4098.

3   2.   M. H. Haider, N. F. Dummer, D. W. Knight, R. L. Jenkins, M. Howard, J. Moulijn,

4   S. H. Taylor and G. J. Hutchings, *Nat. Chem.*, 2015, **7**, 1028-1032.

5   3.   T. Matsumoto, M. Sadakiyo, M. L. Ooi, S. Kitano, T. Yamamoto, S. Matsumura, K.

6   Kato, T. Takeguchi and M. Yamauchi, *Sci. Rep.*, 2014, **4**.

7   4.   T. Matsumoto, M. Sadakiyo, M. L. Ooi, T. Yamamoto, S. Matsumura, K. Kato, T.

8   Takeguchi, N. Ozawa, M. Kubo and M. Yamauchi, *Phys. Chem. Chem. Phys.*, 2015,

9   **17**, 11359-11366.

10   5.   A. Demirbas, *Prog. Energy Combust. Sci.*, 2007, **33**, 1-18.

11   6.   N. Ji, T. Zhang, M. Y. Zheng, A. Q. Wang, H. Wang, X. D. Wang and J. G. G. Chen,

12   *Angew. Chem. Int. Ed.*, 2008, **47**, 8510-8513.

13   7.   E. de Jong, *Avantium, cochair IEA bioenergy Task 42*, 2014, **2**, 11-12.

14   8.   P. Harmsen and M. Hackmann, *Wageningen UR Food & Biobased Research* 2013.

15   9.   H. Kuriyama, *Microbe Engineering Handbook*, 1990.

16   10.   P. Alvira, E. Tomas-Pejo, M. Ballesteros and M. J. Negro, *Bioresour. Technol.*, 2010,

17   **101**, 4851-4861.

18   11.   J. J. Bozell and G. R. Petersen, *Green Chem.*, 2010, **12**, 539-554.

19   12.   T. P. Brewster, A. J. M. Miller, D. M. Heinekey and K. I. Goldberg, *J. Am. Chem.*

20   *Soc.*, 2013, **135**, 16022-16025.

21   13.   H. G. Manyar, C. Paun, R. Pilus, D. W. Rooney, J. M. Thompson and C. Hardacre,

22   *Chem. Commun.*, 2010, **46**, 6279-6281.

23   14.   X. J. Cui, Y. H. Li, C. Topf, K. Junge and M. Beller, *Angew. Chem. Int. Ed.*, 2015,

24   **54**, 10596-10599.

1 15.   M. Naruto and S. Saito, *Nat Commun*, 2015, **6**.

2 16.   J. Seyden-Penne, *Reductions by the Alumino- and Borohydrides in Organic*

3   *Synthesis, 2nd ed.* , 1997.

4 17.   N. M. Yoon, C. S. Pak, H. C. Brown, Krishnam.S and T. P. Stocky, *J. Org. Chem.*,

5   1973, **38**, 2786-2792.

6 18.   A. Pelter, Hutching.Mg, T. E. Levitt and K. Smith, *J. Chem. Soc. Chem. Comm.*,

7   1970, 347-&.

8 19.   V. Gevorgyan, M. Rubin, J. X. Liu and Y. Yamamoto, *J. Org. Chem.*, 2001, **66**,

9   1672-1675.

10 20.   P. A. Dub and T. Ikariya, *Acs Catal*, 2012, **2**, 1718-1741.

11 21.   N. Sakai, K. Kawana, R. Ikeda, Y. Nakaike and T. Konakahara, *Eur. J. Org. Chem.*,

12   2011, 3178-3183.

13 22.   A. Fujishima and K. Honda, *Nature*, 1972, **238**, 37-38.

14 23.   F. Le Formal, N. Tetreault, M. Cornuz, T. Moehl, M. Gratzel and K. Sivula, *Chem.*

15   *Sci.*, 2011, **2**, 737-743.

16 24.   F. Amano, D. Li and B. Ohtani, *Chem. Commun.*, 2010, **46**, 2769-2771.

17 25.   K. Iwashina and A. Kudo, *J. Am. Chem. Soc.*, 2011, **133**, 13272-13275.

18 26.   J. Gu, Y. Yan, J. W. Krizan, Q. D. Gibson, Z. M. Detweiler, R. J. Cava and A. B.

19   Bocarsly, *J. Am. Chem. Soc.*, 2014, **136**, 830-833.

20 27.   D.-D. Qin, Y.-L. Li, T. Wang, Y. Li, X.-Q. Lu, J. Gu, Y.-X. Zhao, Y.-M. Song and

21   C.-L. Tao, *J. Mater. Chem. A*, 2015, **3**, 6751-6755.

22 28.   T. Minegishi, N. Nishimura, J. Kubota and K. Domen, *Chem. Sci.*, 2013, **4**,

23   1120-1124.

24 29.   K. Maeda, M. Higashi, B. Siritanaratkul, R. Abe and K. Domen, *J. Am. Chem. Soc.*,

1   2011, **133**, 12334-12337.

2   30.   M. Higashi, K. Domen and R. Abe, *J. Am. Chem. Soc.*, 2012, **134**, 6968-6971.

3   31.   M. G. Kibria, S. Zhao, F. A. Chowdhury, Q. Wang, H. P. T. Nguyen, M. L. Trudeau,

4   H. Guo and Z. Mi, *Nat Commun*, 2014, **5**.

5   32.   T. Kato, Y. Hakari, S. Ikeda, Q. X. Jia, A. Iwase and A. Kudo, *J. Phys. Chem. Lett.*,

6   2015, **6**, 1042-1047.

7   33.   R. Watanabe, M. Yamauchi, M. Sadakiyo, R. Abe and T. Takeguchi, *Energy Environ.*

8   *Sci.*, 2015, **8**, 1456-1462.

9   34.   F. M. Zhao, F. Yan, Y. Qian, Y. H. Xu and C. Ma, *J. Electroanal. Chem.*, 2013, **698**,

10   31-38.

11   35.   D. J. Pickett and K. S. Yap, *J. Appl. Electrochem.*, 1974, **4**, 17-23.

12   36.   T. Hisatomi, K. Miyazaki, K. Takanabe, K. Maeda, J. Kubota, Y. Sakata and K.

13   Domen, *Chem. Phys. Lett.*, 2010, **486**, 144-146.

14   37.   Y. Sakata, Y. Matsuda, T. Yanagida, K. Hirata, H. Imamura and K. Teramura, *Catal.*

15   *Lett.*, 2008, **125**, 22-26.

16   38.   A. Kudo, K. Omori and H. Kato, *J. Am. Chem. Soc.*, 1999, **121**, 11459-11467.

17   39.   K. Sayama, K. Mukasa, R. Abe, Y. Abe and H. Arakawa, *Chem. Commun.*, 2001,

18   2416-2417.

19   40.   J. Q. Yu and A. Kudo, *Adv. Funct. Mater.*, 2006, **16**, 2163-2169.

20   41.   S. Kitano, N. Murakami, T. Ohno, Y. Mitani, Y. Nosaka, H. Asakura, K. Teramura, T.

21   Tanaka, H. Tada, K. Hashimoto and H. Kominami, *J. Phys. Chem. C*, 2013, **117**,

22   11008-11016.

23   42.   A. Kudo and Y. Miseki, *Chem. Soc. Rev.*, 2009, **38**, 253-278.

24   43.   S. Y. Murakami, H. Kominami, Y. Kera, S. Ikeda, H. Noguchi, K. Uosaki and B.

1   Ohtani, *Res. Chem. Intermed.*, 2007, **33**, 285-296.

2   44.   X. B. Chen, S. H. Shen, L. J. Guo and S. S. Mao, *Chem. Rev.*, 2010, **110**,

3   6503-6570.

4   45.   Y. Q. Liang, T. Tsubota, L. P. A. Mooij and R. van de Krol, *J. Phys. Chem. C*, 2011,

5   **115**, 17594-17598.

6   46.   F. F. Abdi, T. J. Savenije, M. M. May, B. Dam and R. van de Krol, *J. Phys. Chem.*

7   *Lett.*, 2013, **4**, 2752-2757.

8   47.   M. Zhong, T. Hisatomi, Y. B. Kuang, J. Zhao, M. Liu, A. Iwase, Q. X. Jia, H.

9   Nishiyama, T. Minegishi, M. Nakabayashi, N. Shibata, R. Niishiro, C. Katayama, H.

10   Shibano, M. Katayama, A. Kudo, T. Yamada and K. Domen, *J. Am. Chem. Soc.*,

11   2015, **137**, 5053-5060.

12   48.   T. W. Kim and K. S. Choi, *Science*, 2014, **343**, 990-994.

13   49.   N. R. de Tacconi, R. O. Lezna, R. Konduri, F. Ongeri, K. Rajeshwar and F. M.

14   MacDonnell, *Chem-Eur J*, 2005, **11**, 4327-4339.

15   50.   D. E. Scaife, *Sol Energy*, 1980, **25**, 41-54.

16   51.   K. Hashimoto, H. Irie and A. Fujishima, *Jpn J Appl Phys 1*, 2005, **44**, 8269-8285.

17   52.   Y. Nosaka, *Comprehensive Nanoscience and Technology, Vol 1: Nanomaterials*,

18   2011, 571-605.

19   53.   J. Gu, Y. Yan, J. L. Young, K. X. Steirer, N. R. Neale and J. A. Turner, *Nature Mater*,

20   2016, **15**, 456-460.

21

22

4

5   **Figure captions**

6   **Fig. 1** Schematic illustration of light-assisted alcohol electrosynthesis from fossil-free

7   carboxylic acid and water.

8

9   **Fig. 2**   (Upper) Current-voltage curves of electro-reduction of **OX** using a two-electrode

10 system employing a TiO_2 (JRC-TIO-8) cathode in a solution containing **OX** (0.16 M) and a

11 Na_2SO_4 solution (pH 1.2, 40 ml, 0.16 M) and Ga_2O_3, $BiVO_4$ and WO_3 photoanodes in

12 Na_2SO_4 solution (pH 5.8, 40 ml, 0.16 M) at 25 °C under UV-visible light ($\lambda > 200$ nm)

13 irradiation (solid line) or in the dark (broken line). The photographs show photoanodes used

14 for the experiment. (Lower) Schematic illustrations of energy diagrams and photovoltaic

15 performances for the photoanodes under UV-visible light irradiation.

16

17 **Fig. 3** Current-voltage curves of electro-reduction of **OX** using a two-electrode system

18 comprising a TiO_2 (JRC-TIO-7) cathode in solution containing **OX** (0.03 M) and Na_2SO_4

19 solution (pH 1.0, 40 ml, 0.2 M) and a WO_3 photoanode in Na_2SO_4 solution (pH 5.6, 40 ml,

20 0.2 M) under light irradiation, with wavelength >200 nm (red), >300 nm (blue) or >400 nm

21 (black), or in the dark (broken line).

22

23

24

25

Green Chemistry Accepted Manuscript

1   **Fig. 4** Faradaic efficiencies calculated based on the amount of GO and **GC** formed by

2   applying an external bias of 1.0 or 1.5 V in a two-electrode system comprising a TiO_2

3   (JRC-TIO-7) cathode in **OX** solution (pH 1, 40 ml, 0.03 M of OX, 0.2 M Na_2SO_4) and a

4   WO_3 photoanode in Na_2SO_4 solution (pH 5.6, 40 ml, 0.2 M) at 50°C for 2 h under

5   irradiation of UV-visible light with $\lambda > 300$ nm, visible light with $\lambda > 400$ nm or in the

6   dark.

7

8   **Fig. 5** Faradaic efficiencies (FEs) of GO and **GC** production versus the TiO_2 (JRC-TIO-7)

9   cathode potential at 50 °C for 2 h in both the three-electrode system in the dark (square)

10   comprising a TiO_2 cathode and Ag/AgCl reference electrode in a solution containing **OX**

11   (0.03 M) and Na_2SO_4 solution (pH 1.0, 40 ml, 0.2 M) and a Pt anode in a Na_2SO_4 solution

12   (pH 1.0, 40 ml, 0.2 M) and in the two-electrode system comprising a TiO_2 (JRC-TIO-7)

13   cathode in a solution containing **OX** (0.03 M) and Na_2SO_4 solution (pH 1.0, 40 ml, 0.2 M)

14   and a WO_3 photoanode in a Na_2SO_4 solution (pH 1.0, 40 ml, 0.2 M) under irradiation of

15   UV-visible light (triangle) and visible light (circle).
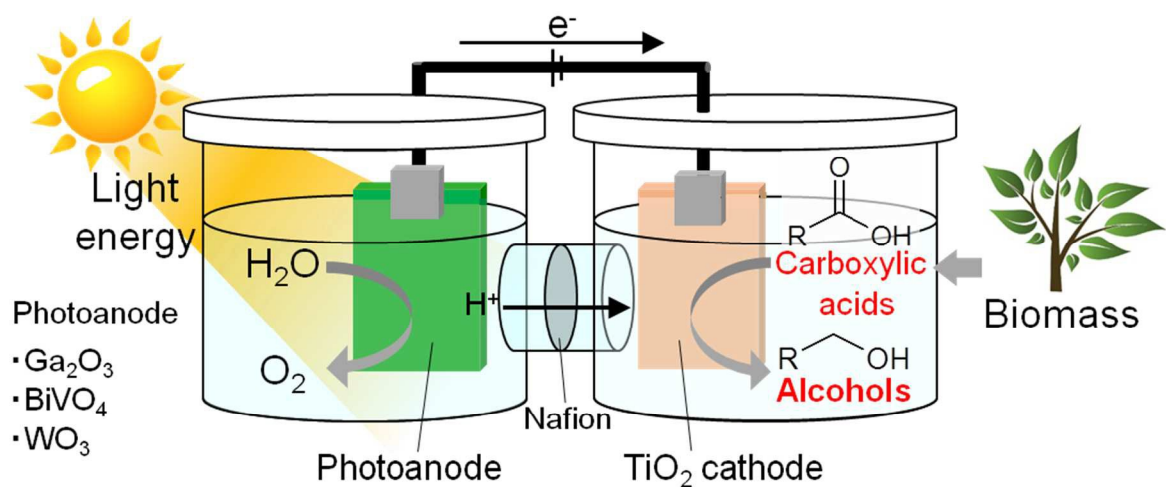
16

17

18

1

2

3 **Fig. 1** Schematic illustration of light-assisted alcohol electrosynthesis from fossil-free
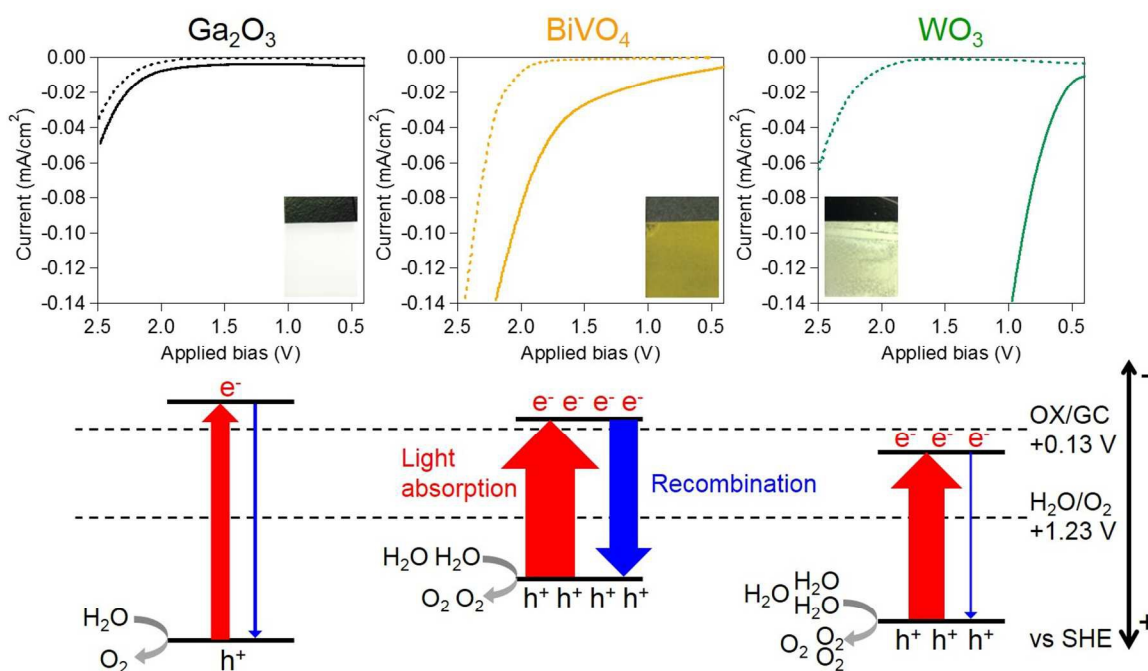
4 carboxylic acid and water.

5

6

Fig. 2 (Upper) Current-voltage curves of electro-reduction of **OX** using a two-electrode system employing a TiO_2 (JRC-TIO-8) cathode in a solution containing **OX** (0.16 M) and a Na_2SO_4 solution (pH 1.2, 40 ml, 0.16 M) and Ga_2O_3, $BiVO_4$ and WO_3 photoanodes in Na_2SO_4 solution (pH 5.8, 40 ml, 0.16 M) at 25 °C under UV-visible light (λ>200 nm) irradiation (solid line) or in the dark (broken line). The photographs show photoanodes used for the experiment. (Lower) Schematic illustrations of energy diagrams and photovoltaic performances for the photoanodes under UV-visible light irradiation.
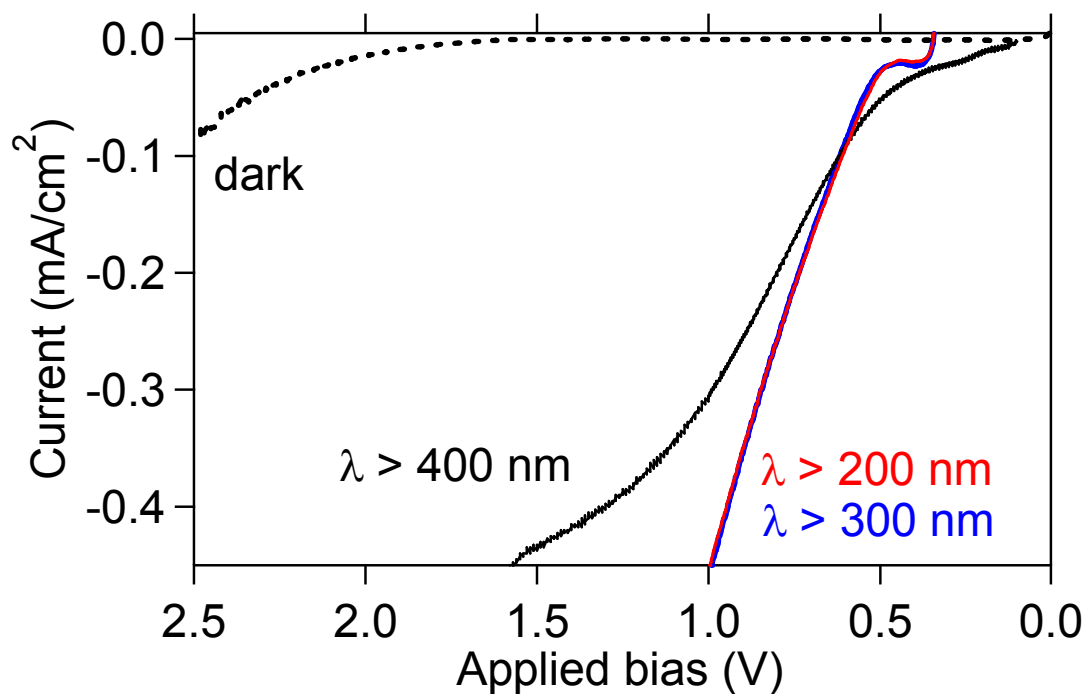
1

2

3   **Fig. 3** Current-voltage curves of electro-reduction of **OX** using a two-electrode system

4   comprising a TiO$_2$ (JRC-TIO-7) cathode in solution containing **OX** (0.03 M) and Na$_2$SO$_4$

5   solution (pH 1.0, 40 ml, 0.2 M) and a WO$_3$ photoanode in Na$_2$SO$_4$ solution (pH 5.6, 40 ml,

6   0.2 M) under light irradiation, with wavelength >200 nm (red), >300 nm (blue) or >400 nm

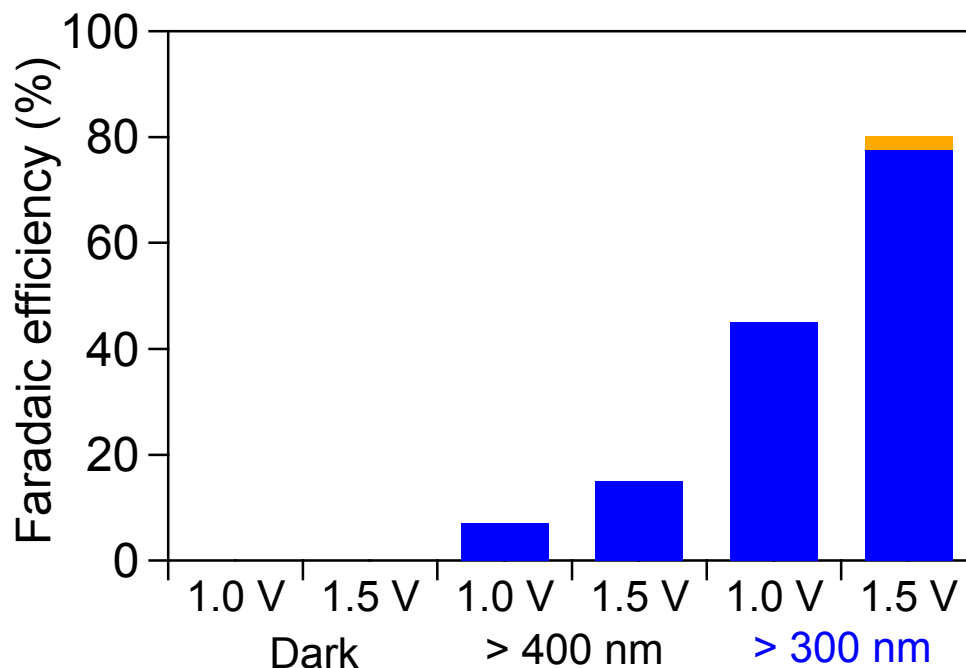7   (black), or in the dark (broken line).

8

1

2

3   **Fig. 4** Faradaic efficiencies calculated based on the amount of GO and **GC** formed by

4   applying an external bias of 1.0 or 1.5 V in a two-electrode system comprising a TiO_2

5   (JRC-TIO-7) cathode in **OX** solution (pH 1, 40 ml, 0.03 M of OX, 0.2 M Na_2SO_4) and a

6   WO_3 photoanode in Na_2SO_4 solution (pH 5.6, 40 ml, 0.2 M) at 50°C for 2 h under

7   irradiation of UV-visible light with $\lambda > 300$ nm, visible light with $\lambda > 400$ nm or in the
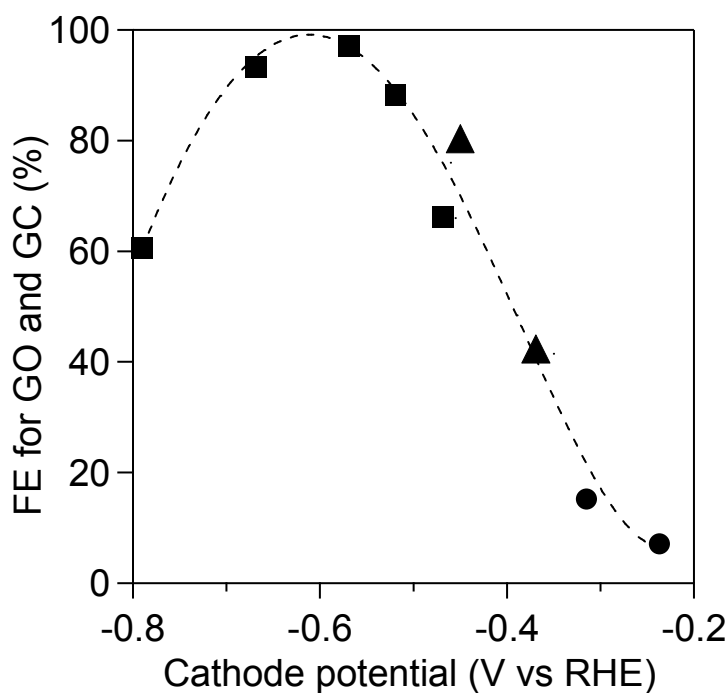
8   dark.

9

Fig. 5 Faradaic efficiencies (FEs) of GO and **GC** production versus the TiO_2 (JRC-TIO-7) cathode potential at 50 °C for 2 h in both the three-electrode system in the dark (square) comprising a TiO_2 cathode and Ag/AgCl reference electrode in a solution containing **OX** (0.03 M) and Na_2SO_4 solution (pH 1.0, 40 ml, 0.2 M) and a Pt anode in a Na_2SO_4 solution (pH 1.0, 40 ml, 0.2 M) and in the two-electrode system comprising a TiO_2 (JRC-TIO-7) cathode in a solution containing **OX** (0.03 M) and Na_2SO_4 solution (pH 1.0, 40 ml, 0.2 M) and a WO_3 photoanode in a Na_2SO_4 solution (pH 1.0, 40 ml, 0.2 M) under irradiation of UV-visible light (triangle) and visible light (circle).

1

2   Graphical abstracts

3